

THE SIGNIFICANCE OF WETTABILITY AND FRACTURE PROPERTIES ON OIL RECOVERY EFFICIENCY IN FRACTURED CARBONATES

Fernø, M.A.¹, Haugen, Å.¹, Graue, A.¹ and Howard, J.J.²

1) Dept. of Physics and Technology, University of Bergen, Norway

2) ConocoPhillips, USA

This paper was prepared for presentation at the International Symposium of the Society of Core Analysts held in Abu Dhabi, UAE 29 October-2 November, 2008

ABSTRACT

Oil recovery mechanisms during waterfloods in fractured carbonate rocks were experimentally investigated using Magnetic Resonance Imaging (MRI). A tortuous fracture network in composite blocks of carbonate rocks was established to investigate the impact of fractures and fracture properties, the sweep efficiency and the impacts from different matrix wettabilities. The average oil production and the *in-situ* fluid saturation development during waterfloods were measured using MRI and then history matched using numerical simulations. Finally, a numerical sensitivity analysis was carried out.

INTRODUCTION

Oil production from water-flooded fractured reservoirs is generally considered to be governed by spontaneous imbibition of water from the water-filled fractures into the matrix blocks, causing the oil to be expelled into the more conductive fractures by counter-current imbibition. The spontaneous imbibition process is heavily dependent on the wettability of the rock, and the properties of the fracture network. It is important to understand the physical processes during the interaction and fluid transfer between matrix and fracture to improve models of multiphase fluid flow in fractured porous media (Gautam and Mohanty, 2004).

We investigated the significance of wettability on sweep efficiency and recovery in experimental waterfloods of fractured outcrop rock samples. The total and local oil recovery and the *in-situ* development of propagating waterfronts at various wettability conditions and in blocks with different fracture properties were considered in this study. Parameter sensitivities studies were performed using a commercially available full-field simulator (Eclipse) to model experimental results from the waterfloods in an ensemble of water-wet and oil-wet blocks. The smaller blocks making up the composite block were separated by a defined fracture network with various apertures and orientations. A 3D numerical representation of each experiment was used to further investigate the influence of fractures on propagating waterfronts during water injection, and to study the significance of fracture properties, such as fracture permeability, on the oil recovery.

EXPERIMENTAL AND NUMERICAL PROCEDURES

The impact of fractures on sweep efficiency during waterflood was experimentally investigated in two outcrop rock types with variable degrees of heterogeneity and wettability preference. The experimental results were reproduced in a numerical simulator by history matching, and sensitivities in the experiment, beyond the experimentally applied parameter settings, were determined. The different steps for both procedures are described below.

Experimental Approach

Two different carbonate rocks, chalk and limestone, at two different wettabilities, strongly water-wet and weakly oil-wet conditions, were used. Each block was waterflooded first as a whole block and then when fractured. The wettability preference was determined by applying similar wettability alteration procedures on core plugs from the same outcrop rock. The term weakly oil-wet in this context refers to an oil-wet state, where a small amount of oil spontaneously imbibes at residual oil saturation, while no spontaneous imbibition of water is observed.

Rock Material

Two different outcrop carbonate rock types provided the rock material for this work.

- Outcrop Rørdal chalk was obtained from the Rørdal outcrop at the Portland cement factory in Ålborg, Denmark. The rock formation was of Maastrichtian age and consisted mainly of coccolith deposits, and the composition was mainly calcite (99%) with some quartz (1%). More details are found in Ekdale and Bromley (1993).
- Outcrop Edwards limestone was obtained from Garden City, Texas, USA. Calcite minerals with mainly moldic pores clearly derived from dissolution of fossils and interparticle porosity. The original interparticle porosity was significantly reduced by re-crystallization of calcite both within and outside these pores. More details are found in Tipura (2008).

Experimental Steps

The experimental procedure is briefly listed below.

1. Cast dry blocks in epoxy. Mount polyoxymethylene (POM) end pieces for up- and downstream connection.
2. Saturate blocks with brine to obtain porosity and measure absolute permeability to brine.
3. Replace brine with deuterium oxide-based brine (D₂O) in a miscible displacement. Measure effluent to ensure a low level of residual brine ($\leq 2\%$ PV).
4. Inject oil at constant pressure drop to establish irreducible water saturation.
5. Age the limestone block using crude oil according to technique described by Graue *et al.* (1999) and Aspenes *et al.* (2003).
6. Replace the crude oil by decalin and decane.

7. Waterflood with deuterium oxide-based brine at constant injection rate while monitoring the *in-situ* saturation development by MRI.
8. Inject oil at constant pressure drop to reestablish irreducible water saturation.
9. Cut and reassemble block according to fracture network, (Figure 1). Apply second coating of epoxy.
10. Waterflood the fractured block with deuterium oxide-based brine at constant injection rate while monitoring the *in-situ* saturation development by MRI.

Numerical Approach

The numerical representation of the rock samples was obtained by reproducing the spatial distribution of porosity variation observed from the 3D MRI images. The permeability distribution was coarsely produced by assuming linear correlation between porosity and permeability, based on a large data set of measurements on core plugs of same rock material. The absolute permeability in the numerical model of the block was verified by explicitly simulating rate and differential pressure relations and calculating permeability from Darcy's law. The main steps during the simulations are listed below. A more detailed description of the numerical simulations is found in Haugen *et al.* (2008).

Numerical Procedures

The numerical procedure is briefly listed below.

1. Represent the whole rock sample numerically. Honor rock properties such as porosity, permeability, pore volume and physical dimensions of the block.
2. Reproduce the experimental conditions including initial fluid saturations, injection rates, boundary and experimental conditions.
3. Match the experimental results in the waterflood of the whole block by adjusting the matrix multiphase functions in the numerical model. Match the average production and the locally observed displacement pattern.
4. For the simulation of the waterflood of the fractured block, leave matrix capillary pressure and relative permeability curves fixed when a satisfactory history match of the whole block has been obtained.
5. Insert the fracture network to the numerical model with explicit fracture representation.
6. Match average production and the *in situ* development of the waterfront in the fractured case by only adjusting the properties of the fracture multiphase functions.

Fracture System

The fractures were created by cutting with a band saw each block into several pieces after re-establishing the irreducible water saturation from the first waterflood step (experimental step 9). The larger block was cut according to the fracture network shown in Figure 1. Each individual piece was stored in decane during cutting to minimize exposure to air. The composite block was rebuilt by placing the smaller blocks according to their original position. Excess fracture space from the thickness of the saw blade was compensated by placing a Teflon spacer in the aperture for the open fracture, thus creating various fracture widths and orientations. Fractures between matrix blocks in contact were referred to as

“closed fractures” (though these are not strictly closed; they still have high permeability and are not a barrier to flow), while one fracture was explicitly held open with a spacer of 1mm thickness and referred to as “open fracture”. The sensitivity of fracture permeability was investigated during a numerical sensitivity study. In this case, it was only the permeability of the closed fractures that was varied, while the permeability of the open fracture was kept high (10^4 mD) and constant.

RESULTS

The reader is referred to Figure 1 for labeling of the smaller blocks making up the composite block during the review of the experimental results. The experimental observations during two waterfloods of fractured rocks are described in detail below, at strongly water-wet and weakly oil-wet conditions. The development of local fluid saturations are depicted in Figure 3 and 4 for the water-wet and oil-wet case, respectively. The numerical results for the experiments are briefly described and compared to the experimental results under Discussion.

Strongly Water-Wet Conditions

The ability to visualize a larger block of rock in the bore of the magnet was investigated in a preliminary flooding test during a miscible brine/D₂O displacement. This test also served as a feasibility study for the calculation of fluid saturation and imaging capability of this new experimental approach.

Miscible Brine/Deuterium Displacement

Deuterium oxide-based (D₂O) brine was used as the aqueous phase to distinguish between the water and oil phase in the MRI. Deuterium brine has the same chemical properties as brine, but the additional neutron in the hydrogen nuclei changes the spin properties of the molecule such that it is not detected, which is exploited in the MRI experimental setup when imaging Hydrogen-bearing fluid phases only. Deuterium brine was injected through a fully brine saturated block while imaging the displacement in three dimensions with MRI. Behind the mixing zone, the MRI signal disappeared rapidly, leaving a residual brine saturation of 2%PV, demonstrated by the D₂O saturation profiles in Figure 2.

Waterflood of Strongly Water-Wet Fractured Block

The *in-situ* oil saturation development during the waterflood of the fractured block is found in the right column of Figure 3 and described in detail below. The injected water entered the lower parts of the inlet of the composite block, and displaced oil upwards along the vertical “closed” fracture. The water saturation remained constant in all other blocks, indicating that the injected water did not cross the fracture. In contrast to the waterflood of the whole block, where water displaced oil in a uniform front, water at this time only advanced in the upper, vertical part of the inlet block, displacing oil from the matrix. Oil was transported via the oil saturated fracture system to the outlet. Just prior to the recovery endpoint in the inlet block, water crossed the lower parts of the “closed” vertical fracture and invaded the lower isolated block. For strongly water-wet conditions this corresponded to the end point for water imbibition, and the capillary pressure at the outlet face of the

block becomes zero. No change in water saturation was observed in the isolated middle block at this time, as this occurred when the water level in the “closed”, vertical fracture at the inlet reached the height of the block. At this time water advanced horizontally in the inlet, isolated lower and middle block simultaneously, but there was no fluid transport or communication between the blocks across the two horizontal “closed” fractures.

Water filled the “open” fracture from the bottom up, simultaneously invading the lower outlet block and displacing oil upwards into the escape fracture in direct contact with the outlet. The production from the upper outlet block was slightly different due to the design of the custom-made end pieces, allowing produced water to spontaneously imbibe back into the block. Water in the “closed” part above the “open” fracture displaced oil horizontally towards the outlet and downwards to the escape fracture at the lower end face of the block. On the opposite side, imbibing water from the outlet end piece displaced oil towards the middle of the block, in the opposite direction, trapping oil in the center of the block.

No significant two-phase production was observed during the waterflood of the fractured water-wet block. Experimental results are listed in Table 2. The development in the average water saturation during waterflood was similar for both the fractured and whole case. The oil recovery mechanism is totally capillary dominated.

Weakly Oil-Wet Conditions

A similar waterflood was conducted in a weakly oil-wet block, with identical fracture network, and the development in water saturation is shown in the right column of Figure 4. Water entered the inlet block across the entire cross-sectional surface of the inlet, with a piston-like displacement associated with a sharp waterfront. No change in oil saturation was observed in any of the other blocks (Figure 1). Water invaded the “closed” fracture before advancing in the upper, horizontal part of the inlet block. Fluid flow predominately took place in the fracture network; once water reached the first fracture it rapidly displaced oil from the fractures, leaving the various matrix blocks upswept. This rapid fracture displacement dynamics could not be properly visualized by the MRI, but the lower “closed” horizontal fracture and the “open” part of the vertical fracture close to the outlet filled with water first.

The oil-wet nature of the blocks prevented imbibition of water from the fracture system to matrix, resulting in poor sweep efficiency, early water breakthrough, and low oil recovery.

DISCUSSION

The results from the waterflood at each wettability state are discussed separately below. The numerical simulations of each displacement generally yielded an excellent match to the experiment, and reproduced the development of propagating waterfronts.

Water-Wet Fractured Rock

The results from the miscible displacement between the brine and deuterium oxide-based brine in Figure 2 are included to demonstrate the applicability of using large-scale blocks in existing MRI experimental laboratory equipment. The results show that the expected decrease in signal intensity in and behind the mixing zone of brine and deuterium oxide brine occurred.

During the waterflood of the fractured block, it was expected that the water-wet block would have high oil recovery, controlled by the strong capillary attraction of water, leading to spontaneous imbibition. The efficiency of the imbibition was also to some degree sensitive to available water flowing through the fractures. No recovery above the spontaneous imbibition potential was observed. This was caused by the lack of a viscous pressure gradient due to direct contact between fractures and the production end. Excellent match between numerical and experimental results was obtained, both with respect to waterflood recovery and the development of the local *in-situ* water saturation development. Using zero fracture capillary pressure in the numerical model successfully reproduced the experimental waterflood of the fractured block.

Oil-Wet Fractured Rock

The waterflood of the oil-wet block yielded low oil recovery due to a combination of unfavorable conditions for spontaneous imbibition of water and the high permeability of the fracture system. The high permeability limited the viscous gradient in the injecting water needed to overcome the entry capillary pressure for water to enter the isolated matrix blocks. This led to very poor recovery as the injected water moved straight from the inlet block into the fracture system and was produced at the outlet end. The production of oil was much lower than in the waterflood at whole block conditions and to the equivalent waterflood in the strongly water-wet chalk block with the same fracture network. The displacement pattern was also very different due to the change in matrix wettability. The numerical simulations successfully matched the experimentally observed developments of *in-situ* water saturation during the waterflood of the fractured block. Zero capillary pressure in the fractures reproduced the spatially sweep observed with the MRI.

Impacts of Fracture Permeability on Oil Recovery and Sweep Efficiency

In addition to reproducing the experimental results during both waterfloods at water-wet and oil-wet conditions, the numerical model was used to study sensitivities of some of the physical parameters in the experiments. The fracture/matrix permeability ratio was investigated, to identify the required reduction in fracture permeability to obtain a ratio allowing water diversion into the matrices. The permeability of fractures may over geological time be reduced naturally by diagenesis and cementation, or artificially in a production scenario by e.g. polymer or foam. The amount of water forced from the fracture into the matrix will also depend on the wettability of the rock. Only the permeability of the “closed” fractures, where matrix surfaces were in contact, was altered in the numerical sensitivity study. The permeability of the “open” fracture was kept high (10^4 mD) and constant. The results are shown in Figure 5, where the potential for improved oil recovery

was largest for the oil-wet case, as recovery in the strongly water-wet case was not sensitive to fracture permeability. Moderately water-wet experimental data in chalk reported by Graue *et al.* (2002) are included. Reducing the permeability to about 20 times the matrix permeability we saw that a significant pressure gradient starts to form. This in turn created a viscous pressure drop across the different matrix blocks and water may displace the oil by viscous forces. The oil recovery in the water-wet case was strongly capillary dominated and was not expected to be significantly affected by fracture permeability.

CONCLUSIONS

- The applicability of using large, epoxy coated rock samples in existing MRI laboratory equipment was demonstrated, which initiated a series of waterflood experiments in samples larger than standard core plugs.
- The significance of wettability on oil recovery from fractured rock was demonstrated by waterflooding the same fracture network in two blocks with different wettabilities; one water-wet and one oil-wet.
- The impact from fractures on propagating waterfronts during waterfloods was identified by performing waterfloods at different states in each block; first whole, then when fractured.
- The local fluid saturation development was successfully imaged using MRI.
- A numerical model of the experiment was created, honoring the spatial distribution of porosity, permeability, fractures and wettability in both homogeneous and heterogeneous rock types.
- Multiphase functions such as capillary pressure and relative permeability were found by matching both the local fluid development and average values during waterfloods at non-fractured conditions.
- Fractures were explicitly represented in the numerical model, with explicit porosity, permeability and two-phase functions and shown to have significant impacts on oil recovery.
- The permeability of the narrow fractures was changed in a sensitivity study on the ratio between fracture and matrix permeability. It was found that matrix wettability and fracture permeability have significant impacts on the improved oil recovery potential.

ACKNOWLEDGEMENTS

Two of the authors are indebted to the Royal Norwegian Research Council for financial support. The authors are grateful to ConocoPhillips for permission to publish this work. Reviewers Jill Buckley and Ted Braun are thanked for their contributions.

REFERENCES

Aspenes, E., Graue, A. and Ramsdal, J. "*In situ wettability distribution and wetting stability in outcrop chalk aged in crude oil*", Journal of Petroleum Science and Engineering **39**(3-4):pp.337-350, 2003

- Ekdale, A.A. and Bromley, R.G. "Trace Fossils and Ichnofabric in the Kjølby Gaard Marl, Uppermost Cretaceous, Denmark", *Bull Geol. Soc. Denmark* **31**:pp.107-119, 1993
- Gautam, P.S. and Mohanty, K.K. "Matrix-Fracture Transfer through Countercurrent Imbibition in Presence of Fracture Fluid Flow", *Transport in Porous Media* **55**(3):pp.309-337, 2004
- Graue, A., Viksund, B.G., Eilertsen, T. and Moe, R. "Systematic wettability alteration by aging sandstone and carbonate rock in crude oil", *Journal of Petroleum Science and Engineering* **24**(2-4):pp.85-97, 1999
- Graue, A., Nesse, K., Baldwin, B.A., Spinler, E.A. and Tobola, D. "Impact of Fracture Permeability on Oil Recovery in Moderately Water-Wet Fractured Chalk Reservoirs", SPE/DOE Improved Oil Recovery Symposium, Tulsa, OK, USA, April 17-19, 2002
- Haugen, Å., Fernø, M.A. and Graue, A. "Numerical simulation and sensitivity analysis of in-situ fluid flow in MRI laboratory waterfloods of fractured carbonate rocks at different wettabilities", SPE ATCE, Denver, CO, USA, September 21-24, 2008
- Tipura, L. "Wettability Characterization by NMR T2 Measurements in Edwards Limestone" Master Thesis, Dept. of Physics and Technology, University of Bergen, Bergen, Norway, 2008

Table 1. Rock Properties

	Height [cm]	Length [cm]	Width [cm]	Porosity	Permeability [mD]
Chalk	8.4	13.2	2.4	0.48	3.2
Limestone	8.0	15.9	2.5	0.24	23.4

Table 2. Experimental Results Fracture Waterflood

	Injection Rate [cc/h]	Production condition	Initial S_w	Final S_w	ΔS_w	Water breakthrough [PV injected]
Chalk (Water-wet)	5.0	Const.pressure (atmospheric)	0.26	0.58	0.32	0.52
Limestone (Oil-wet)	2.0	Const.pressure (atmospheric)	0.30	0.41	0.11	0.27

Table 3. Waterflood Recovery Results

Recovery Factor [%OOIP]	Water-Wet		Oil-Wet	
	Experiment	Numerical	Experiment	Numerical
Whole Block	50	48.7	70.0	70.0
Fractured Block	44.6	48.6	15.7	16.4

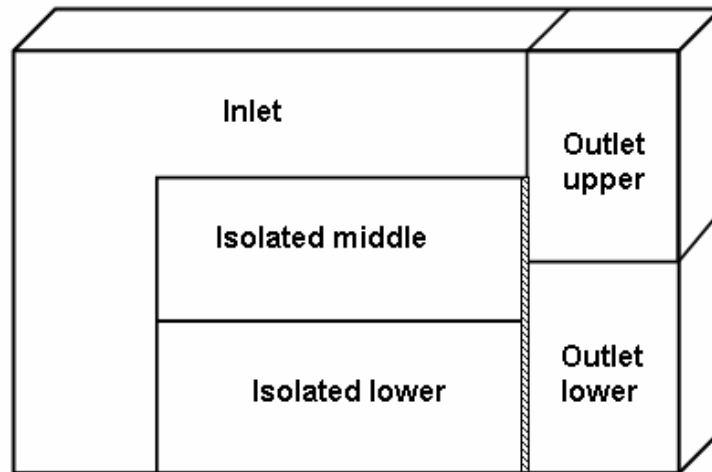



Figure 1. A schematic showing the composite block and the artificially created fracture configuration created. The actual dimensions of each block vary with each experiment.
 indicates that the fracture is open with a 1mm aperture.

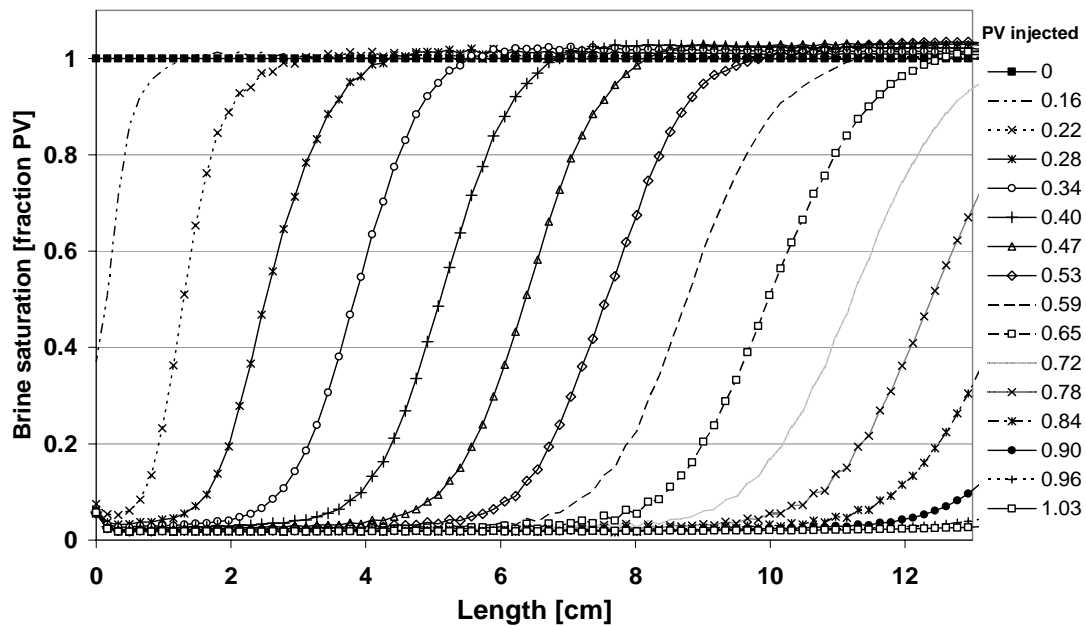


Figure 2. One dimensional brine saturation profile during the concentration of brine during the miscible displacement between brine and deuterium brine. The concentration of brine behind the mixing front rapidly decreases to a residual saturation of about 2%PV. A residual brine saturation of about 2%PV after 1PV injected deuterium brine.

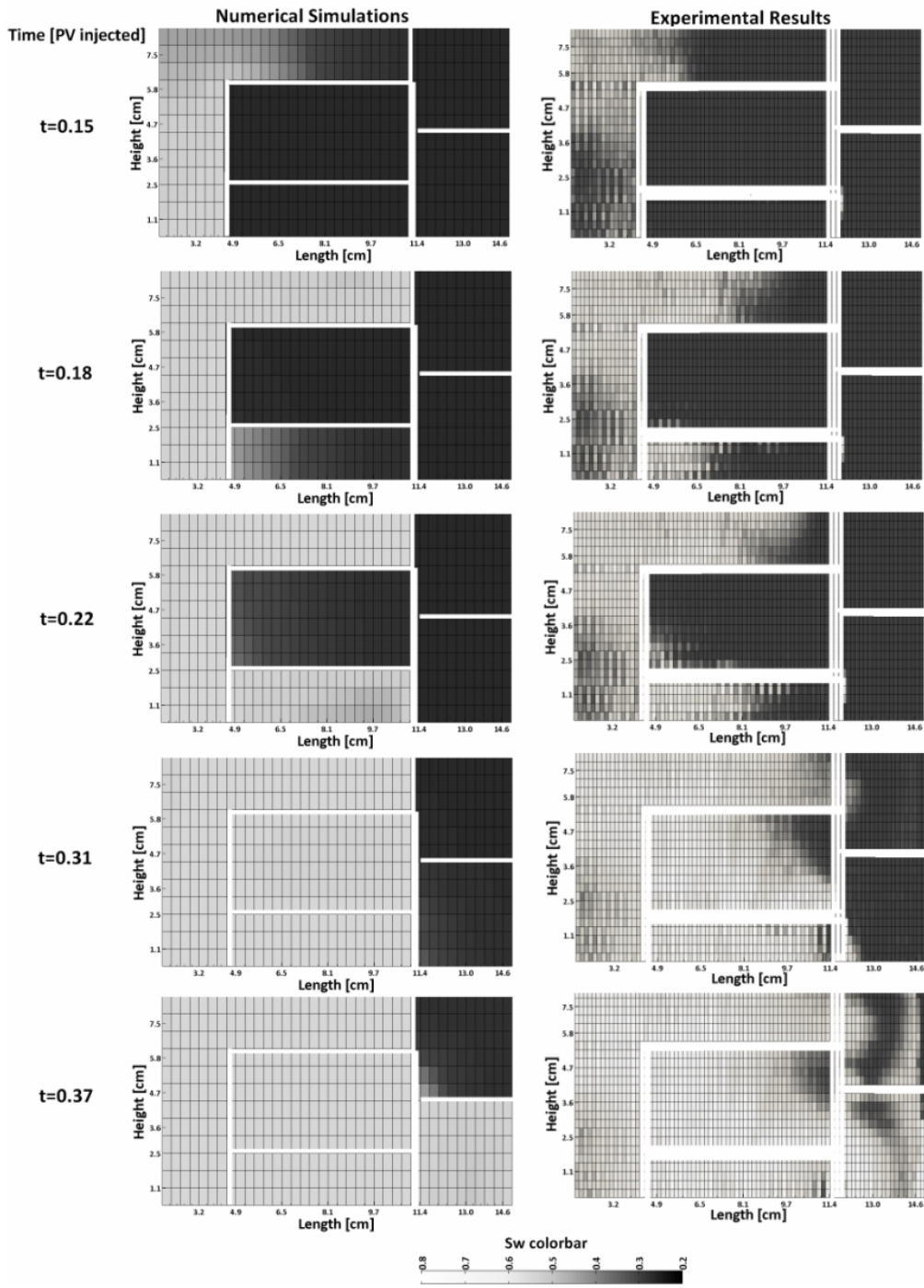


Figure 3. Waterflood of the strongly water-wet composite chalk block at five different pore volume injected. The displacement process is capillary dominated, characterized by high recovery and excellent sweep efficiency.

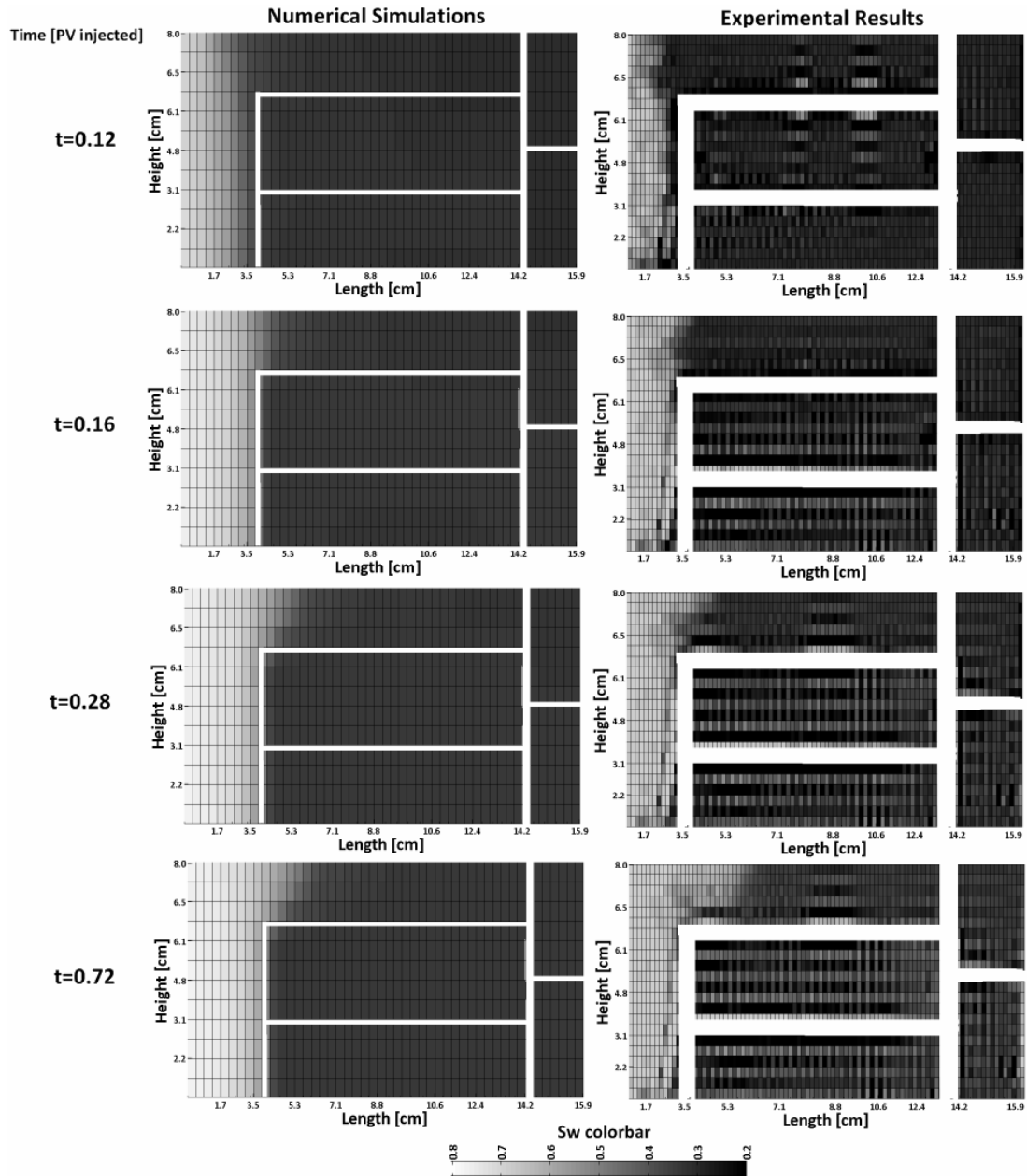


Figure 4. Waterflood of the weakly oil-wet composite limestone block at different pore volumes injected. The recovery of oil is low with early water breakthrough, poor sweep associated with no water imbibition from surrounding fracture network into isolated matrix blocks. Small difference in matrix water saturation when water reaches the fractures, compare $t=0.28$ and $t=0.72$ PV injected, i.e. the injected water flows primarily through fractures to outlet without displacing oil.

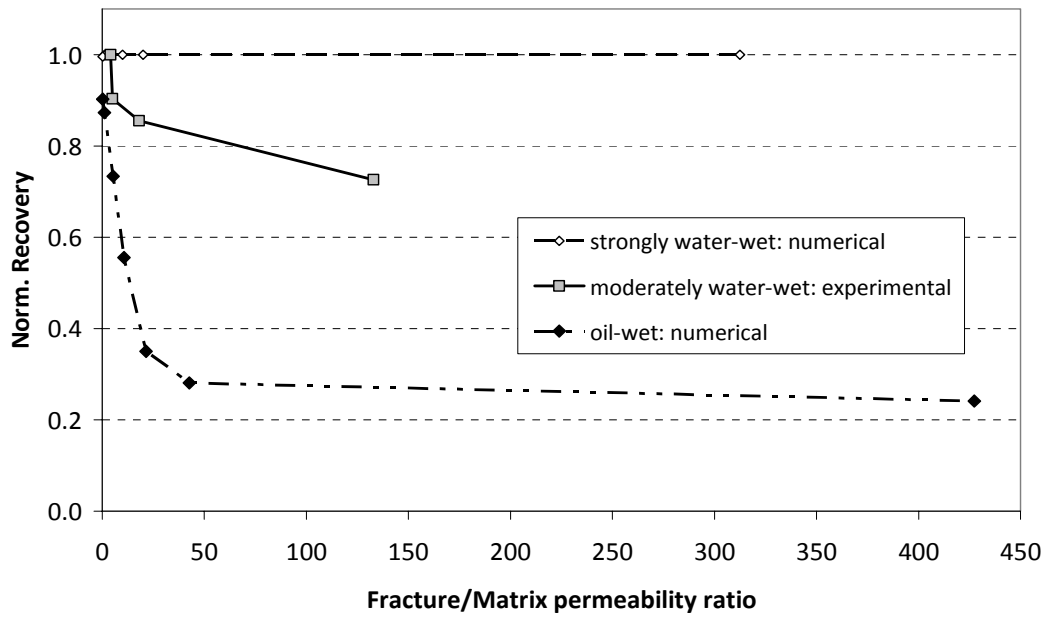


Figure 5. Waterflood recovery as a function of fracture/matrix permeability ratio. The potential for improved oil recovery is largest for the oil-wet case, as recovery in the strongly water-wet case is not sensitive to fracture permeability.